

Search for Hadronic Decays of a Light Higgs Boson in the Radiative Decay $\Upsilon \rightarrow \gamma A^0$

J. P. Lees,¹ V. Poireau,¹ V. Tisserand,¹ J. Garra Tico,² E. Grauges,² M. Martinelli,^{3a,3b} D. A. Milanes,^{3a} A. Palano,^{3a,3b} M. Pappagallo,^{3a,3b} G. Eigen,⁴ B. Stugu,⁴ D. N. Brown,⁵ L. T. Kerth,⁵ Yu. G. Kolomensky,⁵ G. Lynch,⁵ H. Koch,⁶ T. Schroeder,⁶ D. J. Asgeirsson,⁷ C. Hearty,⁷ T. S. Mattison,⁷ J. A. McKenna,⁷ R. Y. So,⁷ A. Khan,⁸ V. E. Blinov,⁹ A. R. Buzykaev,⁹ V. P. Druzhinin,⁹ V. B. Golubev,⁹ E. A. Kravchenko,⁹ A. P. Onuchin,⁹ S. I. Serednyakov,⁹ Yu. I. Skovpen,⁹ E. P. Solodov,⁹ K. Yu. Todyshev,⁹ A. N. Yushkov,⁹ M. Bondioli,¹⁰ D. Kirkby,¹⁰ A. J. Lankford,¹⁰ M. Mandelkern,¹⁰ D. P. Stoker,¹⁰ H. Atmacan,¹¹ J. W. Gary,¹¹ F. Liu,¹¹ O. Long,¹¹ G. M. Vitug,¹¹ C. Campagnari,¹² T. M. Hong,¹² D. Kovalskiy,¹² J. D. Richman,¹² C. A. West,¹² A. M. Eisner,¹³ J. Kroseberg,¹³ W. S. Lockman,¹³ A. J. Martinez,¹³ T. Schalk,¹³ B. A. Schumm,¹³ A. Seiden,¹³ C. H. Cheng,¹⁴ D. A. Doll,¹⁴ B. Echenard,¹⁴ K. T. Flood,¹⁴ D. G. Hitlin,¹⁴ P. Ongmongkolkul,¹⁴ F. C. Porter,¹⁴ A. Y. Rakitin,¹⁴ R. Andreassen,¹⁵ M. S. Dubrovin,¹⁵ Z. Huard,¹⁵ B. T. Meadows,¹⁵ M. D. Sokoloff,¹⁵ L. Sun,¹⁵ P. C. Bloom,¹⁶ W. T. Ford,¹⁶ A. Gaz,¹⁶ M. Nagel,¹⁶ U. Nauenberg,¹⁶ J. G. Smith,¹⁶ S. R. Wagner,¹⁶ R. Ayad,^{17,*} W. H. Toki,¹⁷ B. Spaan,¹⁸ M. J. Kobel,¹⁹ K. R. Schubert,¹⁹ R. Schwierz,¹⁹ D. Bernard,²⁰ M. Verderi,²⁰ P. J. Clark,²¹ S. Playfer,²¹ D. Bettoni,^{22a} C. Bozzi,^{22a} R. Calabrese,^{22a,22b} G. Cibinetto,^{22a,22b} E. Fioravanti,^{22a,22b} I. Garzia,^{22a,22b} E. Luppi,^{22a,22b} M. Munerato,^{22a,22b} M. Negrini,^{22a,22b} L. Piemontese,^{22a} V. Santoro,^{22a} R. Baldini-Ferrolì,²³ A. Calcaterra,²³ R. de Sangro,²³ G. Finocchiaro,²³ M. Nicolaci,²³ P. Patteri,²³ I. M. Peruzzi,^{23,†} M. Piccolo,²³ M. Rama,²³ A. Zallo,²³ R. Contri,^{24a,24b} E. Guido,^{24a,24b} M. Lo Vetere,^{24a,24b} M. R. Monge,^{24a,24b} S. Passaggio,^{24a} C. Patrignani,^{24a,24b} E. Robutti,^{24a} B. Bhuyan,²⁵ V. Prasad,²⁵ C. L. Lee,²⁶ M. Morii,²⁶ A. J. Edwards,²⁷ A. Adametz,²⁸ J. Marks,²⁸ U. Uwer,²⁸ F. U. Bernlochner,²⁹ M. Ebert,²⁹ H. M. Lacker,²⁹ T. Lueck,²⁹ P. D. Dauncey,³⁰ M. Tibbetts,³⁰ P. K. Behera,³¹ U. Mallik,³¹ C. Chen,³² J. Cochran,³² W. T. Meyer,³² S. Prell,³² E. I. Rosenberg,³² A. E. Rubin,³² A. V. Gritsan,³³ Z. J. Guo,³³ N. Arnaud,³⁴ M. Davier,³⁴ G. Grosdidier,³⁴ F. Le Diberder,³⁴ A. M. Lutz,³⁴ B. Malaescu,³⁴ P. Roudeau,³⁴ M. H. Schune,³⁴ A. Stocchi,³⁴ G. Wormser,³⁴ D. J. Lange,³⁵ D. M. Wright,³⁵ I. Bingham,³⁶ C. A. Chavez,³⁶ J. P. Coleman,³⁶ J. R. Fry,³⁶ E. Gabathuler,³⁶ D. E. Hutchcroft,³⁶ D. J. Payne,³⁶ C. Touramanis,³⁶ A. J. Bevan,³⁷ F. Di Lodovico,³⁷ R. Sacco,³⁷ M. Sigamani,³⁷ G. Cowan,³⁸ D. N. Brown,³⁹ C. L. Davis,³⁹ A. G. Denig,⁴⁰ M. Fritsch,⁴⁰ W. Gradl,⁴⁰ A. Hafner,⁴⁰ E. Prencipe,⁴⁰ K. E. Alwyn,⁴¹ D. Bailey,⁴¹ R. J. Barlow,^{41,‡} G. Jackson,⁴¹ G. D. Lafferty,⁴¹ E. Behn,⁴² R. Cenci,⁴² B. Hamilton,⁴² A. Jawahery,⁴² D. A. Roberts,⁴² G. Simi,⁴² C. Dallapiccola,⁴³ R. Cowan,⁴⁴ D. Dujmic,⁴⁴ G. Sciolla,⁴⁴ D. Lindemann,⁴⁵ P. M. Patel,⁴⁵ S. H. Robertson,⁴⁵ M. Schram,⁴⁵ P. Biassoni,^{46a,46b} A. Lazzaro,^{46a,46b} V. Lombardo,^{46a} N. Neri,^{46a,46b} F. Palombo,^{46a,46b} S. Stracka,^{46a,46b} L. Cremaldi,⁴⁷ R. Godang,^{47,§} R. Kroeger,⁴⁷ P. Sonnek,⁴⁷ D. J. Summers,⁴⁷ X. Nguyen,⁴⁸ P. Taras,⁴⁸ G. De Nardo,^{49a,49b} D. Monorchio,^{49a,49b} G. Onorato,^{49a,49b} C. Sciacca,^{49a,49b} G. Raven,⁵⁰ H. L. Snoek,⁵⁰ C. P. Jessop,⁵¹ K. J. Knoepfel,⁵¹ J. M. LoSecco,⁵¹ W. F. Wang,⁵¹ K. Honscheid,⁵² R. Kass,⁵² J. Brau,⁵³ R. Frey,⁵³ N. B. Sinev,⁵³ D. Strom,⁵³ E. Torrence,⁵³ E. Feltresi,^{54a,54b} N. Gagliardi,^{54a,54b} M. Margoni,^{54a,54b} M. Morandin,^{54a} M. Posocco,^{54a} M. Rotondo,^{54a} F. Simonetto,^{54a,54b} R. Stroili,^{54a,54b} S. Akar,⁵⁵ E. Ben-Haim,⁵⁵ M. Bomben,⁵⁵ G. R. Bonneaud,⁵⁵ H. Briand,⁵⁵ G. Calderini,⁵⁵ J. Chauveau,⁵⁵ O. Hamon,⁵⁵ Ph. Leruste,⁵⁵ G. Marchiori,⁵⁵ J. Ocariz,⁵⁵ S. Sitt,⁵⁵ M. Biasini,^{56a,56b} E. Manoni,^{56a,56b} S. Pacetti,^{56a,56b} A. Rossi,^{56a,56b} C. Angelini,^{57a,57b} G. Batignani,^{57a,57b} S. Bettarini,^{57a,57b} M. Carpinelli,^{57a,57b,||} G. Casarosa,^{57a,57b} A. Cervelli,^{57a,57b} F. Forti,^{57a,57b} M. A. Giorgi,^{57a,57b} A. Lusiani,^{57a,57c} B. Oberhof,^{57a,57b} E. Paoloni,^{57a,57b} A. Perez,^{57a} G. Rizzo,^{57a,57b} J. J. Walsh,^{57a} D. Lopes Pegna,⁵⁸ C. Lu,⁵⁸ J. Olsen,⁵⁸ A. J. S. Smith,⁵⁸ A. V. Telnov,⁵⁸ F. Anulli,^{59a} G. Cavoto,^{59a} R. Faccini,^{59a,59b} F. Ferrarotto,^{59a} F. Ferroni,^{59a,59b} M. Gaspero,^{59a,59b} L. Li Gioi,^{59a} M. A. Mazzoni,^{59a} G. Piredda,^{59a} C. Büniger,⁶⁰ O. Grünberg,⁶⁰ T. Hartmann,⁶⁰ T. Leddig,⁶⁰ H. Schröder,⁶⁰ R. Waldi,⁶⁰ T. Adye,⁶¹ E. O. Olaiya,⁶¹ F. F. Wilson,⁶¹ S. Emery,⁶² G. Hamel de Monchenault,⁶² G. Vasseur,⁶² Ch. Yèche,⁶² D. Aston,⁶³ D. J. Bard,⁶³ R. Bartoldus,⁶³ J. F. Benitez,⁶³ C. Cartaro,⁶³ M. R. Convery,⁶³ J. Dorfan,⁶³ G. P. Dubois-Felsmann,⁶³ W. Dunwoodie,⁶³ R. C. Field,⁶³ M. Franco Sevilla,⁶³ B. G. Fulsom,⁶³ A. M. Gabareen,⁶³ M. T. Graham,⁶³ P. Grenier,⁶³ C. Hast,⁶³ W. R. Innes,⁶³ M. H. Kelsey,⁶³ H. Kim,⁶³ P. Kim,⁶³ M. L. Kocian,⁶³ D. W. G. S. Leith,⁶³ P. Lewis,⁶³ S. Li,⁶³ B. Lindquist,⁶³ S. Luitz,⁶³ V. Luth,⁶³ H. L. Lynch,⁶³ D. B. MacFarlane,⁶³ D. R. Muller,⁶³ H. Neal,⁶³ S. Nelson,⁶³ I. Ofte,⁶³ M. Perl,⁶³ T. Pulliam,⁶³ B. N. Ratcliff,⁶³ A. Roodman,⁶³ A. A. Salnikov,⁶³ R. H. Schindler,⁶³ A. Snyder,⁶³ D. Su,⁶³ M. K. Sullivan,⁶³ J. Va'vra,⁶³ A. P. Wagner,⁶³ M. Weaver,⁶³ W. J. Wisniewski,⁶³ M. Wittgen,⁶³ D. H. Wright,⁶³ H. W. Wulsin,⁶³ A. K. Yarritu,⁶³ C. C. Young,⁶³ V. Ziegler,⁶³ W. Park,⁶⁴ M. V. Purohit,⁶⁴ R. M. White,⁶⁴ J. R. Wilson,⁶⁴ A. Randle-Conde,⁶⁵ S. J. Sekula,⁶⁵ M. Bellis,⁶⁶ P. R. Burchat,⁶⁶ T. S. Miyashita,⁶⁶ M. S. Alam,⁶⁷ J. A. Ernst,⁶⁷ R. Gorodeisky,⁶⁸ N. Guttman,⁶⁸ D. R. Peimer,⁶⁸ A. Soffer,⁶⁸ P. Lund,⁶⁹ S. M. Spanier,⁶⁹ R. Eckmann,⁷⁰ J. L. Ritchie,⁷⁰ A. M. Ruland,⁷⁰ C. J. Schilling,⁷⁰ R. F. Schwitters,⁷⁰ B. C. Wray,⁷⁰ J. M. Izen,⁷¹ X. C. Lou,⁷¹ F. Bianchi,^{72a,72b}

D. Gamba,^{72a,72b} L. Lanceri,^{73a,73b} L. Vitale,^{73a,73b} F. Martinez-Vidal,⁷⁴ A. Oyanguren,⁷⁴ H. Ahmed,⁷⁵ J. Albert,⁷⁵ Sw. Banerjee,⁷⁵ H. H. F. Choi,⁷⁵ G. J. King,⁷⁵ R. Kowalewski,⁷⁵ M. J. Lewczuk,⁷⁵ I. M. Nugent,⁷⁵ J. M. Roney,⁷⁵ R. J. Sobie,⁷⁵ N. Tasneem,⁷⁵ T. J. Gershon,⁷⁶ P. F. Harrison,⁷⁶ T. E. Latham,⁷⁶ E. M. T. Puccio,⁷⁶ H. R. Band,⁷⁷ S. Dasu,⁷⁷ Y. Pan,⁷⁷ R. Prepost,⁷⁷ and S. L. Wu⁷⁷

(BABAR Collaboration)

- ¹Laboratoire d'Annecy-le-Vieux de Physique des Particules (LAPP), Université de Savoie, CNRS/IN2P3, F-74941 Annecy-Le-Vieux, France
- ²Universitat de Barcelona, Facultat de Física, Departament ECM, E-08028 Barcelona, Spain
- ^{3a}INFN Sezione di Bari, I-70126 Bari, Italy
- ^{3b}Dipartimento di Fisica, Università di Bari, I-70126 Bari, Italy
- ⁴University of Bergen, Institute of Physics, N-5007 Bergen, Norway
- ⁵Lawrence Berkeley National Laboratory and University of California, Berkeley, California 94720, USA
- ⁶Ruhr Universität Bochum, Institut für Experimentalphysik 1, D-44780 Bochum, Germany
- ⁷University of British Columbia, Vancouver, British Columbia, Canada V6T 1Z1
- ⁸Brunel University, Uxbridge, Middlesex UB8 3PH, United Kingdom
- ⁹Budker Institute of Nuclear Physics, Novosibirsk 630090, Russia
- ¹⁰University of California at Irvine, Irvine, California 92697, USA
- ¹¹University of California at Riverside, Riverside, California 92521, USA
- ¹²University of California at Santa Barbara, Santa Barbara, California 93106, USA
- ¹³University of California at Santa Cruz, Institute for Particle Physics, Santa Cruz, California 95064, USA
- ¹⁴California Institute of Technology, Pasadena, California 91125, USA
- ¹⁵University of Cincinnati, Cincinnati, Ohio 45221, USA
- ¹⁶University of Colorado, Boulder, Colorado 80309, USA
- ¹⁷Colorado State University, Fort Collins, Colorado 80523, USA
- ¹⁸Technische Universität Dortmund, Fakultät Physik, D-44221 Dortmund, Germany
- ¹⁹Technische Universität Dresden, Institut für Kern- und Teilchenphysik, D-01062 Dresden, Germany
- ²⁰Laboratoire Leprince-Ringuet, Ecole Polytechnique, CNRS/IN2P3, F-91128 Palaiseau, France
- ²¹University of Edinburgh, Edinburgh EH9 3JZ, United Kingdom
- ^{22a}INFN Sezione di Ferrara, I-44100 Ferrara, Italy
- ^{22b}Dipartimento di Fisica, Università di Ferrara, I-44100 Ferrara, Italy
- ²³INFN Laboratori Nazionali di Frascati, I-00044 Frascati, Italy
- ^{24a}INFN Sezione di Genova, I-16146 Genova, Italy
- ^{24b}Dipartimento di Fisica, Università di Genova, I-16146 Genova, Italy
- ²⁵Indian Institute of Technology Guwahati, Guwahati, Assam, 781 039, India
- ²⁶Harvard University, Cambridge, Massachusetts 02138, USA
- ²⁷Harvey Mudd College, Claremont, California 91711
- ²⁸Universität Heidelberg, Physikalisches Institut, Philosophenweg 12, D-69120 Heidelberg, Germany
- ²⁹Humboldt-Universität zu Berlin, Institut für Physik, Newtonstr. 15, D-12489 Berlin, Germany
- ³⁰Imperial College London, London, SW7 2AZ, United Kingdom
- ³¹University of Iowa, Iowa City, Iowa 52242, USA
- ³²Iowa State University, Ames, Iowa 50011-3160, USA
- ³³Johns Hopkins University, Baltimore, Maryland 21218, USA
- ³⁴Laboratoire de l'Accélérateur Linéaire, IN2P3/CNRS et Université Paris-Sud 11, Centre Scientifique d'Orsay, Boîte Postale 34, F-91898 Orsay Cedex, France
- ³⁵Lawrence Livermore National Laboratory, Livermore, California 94550, USA
- ³⁶University of Liverpool, Liverpool L69 7ZE, United Kingdom
- ³⁷Queen Mary, University of London, London, E1 4NS, United Kingdom
- ³⁸University of London, Royal Holloway and Bedford New College, Egham, Surrey TW20 0EX, United Kingdom
- ³⁹University of Louisville, Louisville, Kentucky 40292, USA
- ⁴⁰Johannes Gutenberg-Universität Mainz, Institut für Kernphysik, D-55099 Mainz, Germany
- ⁴¹University of Manchester, Manchester M13 9PL, United Kingdom
- ⁴²University of Maryland, College Park, Maryland 20742, USA
- ⁴³University of Massachusetts, Amherst, Massachusetts 01003, USA
- ⁴⁴Massachusetts Institute of Technology, Laboratory for Nuclear Science, Cambridge, Massachusetts 02139, USA
- ⁴⁵McGill University, Montréal, Québec, Canada H3A 2T8
- ^{46a}INFN Sezione di Milano, I-20133 Milano, Italy
- ^{46b}Dipartimento di Fisica, Università di Milano, I-20133 Milano, Italy

- ⁴⁷University of Mississippi, University, Mississippi 38677, USA
⁴⁸Université de Montréal, Physique des Particules, Montréal, Québec, Canada H3C 3J7
^{49a}INFN Sezione di Napoli, I-80126 Napoli, Italy
^{49b}Dipartimento di Scienze Fisiche, Università di Napoli Federico II, I-80126 Napoli, Italy
⁵⁰NIKHEF, National Institute for Nuclear Physics and High Energy Physics, NL-1009 DB Amsterdam, The Netherlands
⁵¹University of Notre Dame, Notre Dame, Indiana 46556, USA
⁵²Ohio State University, Columbus, Ohio 43210, USA
⁵³University of Oregon, Eugene, Oregon 97403, USA
^{54a}INFN Sezione di Padova, I-35131 Padova, Italy
^{54b}Dipartimento di Fisica, Università di Padova, I-35131 Padova, Italy
⁵⁵Laboratoire de Physique Nucléaire et de Hautes Energies, IN2P3/CNRS, Université Pierre et Marie Curie-Paris6, Université Denis Diderot-Paris7, F-75252 Paris, France
^{56a}INFN Sezione di Perugia, I-06100 Perugia, Italy
^{56b}Dipartimento di Fisica, Università di Perugia, I-06100 Perugia, Italy
^{57a}INFN Sezione di Pisa, I-56127 Pisa, Italy
^{57b}Dipartimento di Fisica, Università di Pisa, I-56127 Pisa, Italy
^{57c}Scuola Normale Superiore di Pisa, I-56127 Pisa, Italy
⁵⁸Princeton University, Princeton, New Jersey 08544, USA
^{59a}INFN Sezione di Roma, I-00185 Roma, Italy
^{59b}Dipartimento di Fisica, Università di Roma La Sapienza, I-00185 Roma, Italy
⁶⁰Universität Rostock, D-18051 Rostock, Germany
⁶¹Rutherford Appleton Laboratory, Chilton, Didcot, Oxon, OX11 0QX, United Kingdom
⁶²CEA, Irfu, SPP, Centre de Saclay, F-91191 Gif-sur-Yvette, France
⁶³SLAC National Accelerator Laboratory, Stanford, California 94309 USA
⁶⁴University of South Carolina, Columbia, South Carolina 29208, USA
⁶⁵Southern Methodist University, Dallas, Texas 75275, USA
⁶⁶Stanford University, Stanford, California 94305-4060, USA
⁶⁷State University of New York, Albany, New York 12222, USA
⁶⁸Tel Aviv University, School of Physics and Astronomy, Tel Aviv, 69978, Israel
⁶⁹University of Tennessee, Knoxville, Tennessee 37996, USA
⁷⁰University of Texas at Austin, Austin, Texas 78712, USA
⁷¹University of Texas at Dallas, Richardson, Texas 75083, USA
^{72a}INFN Sezione di Torino, I-10125 Torino, Italy
^{72b}Dipartimento di Fisica Sperimentale, Università di Torino, I-10125 Torino, Italy
^{73a}INFN Sezione di Trieste, I-34127 Trieste, Italy
^{73b}Dipartimento di Fisica, Università di Trieste, I-34127 Trieste, Italy
⁷⁴IFIC, Universitat de Valencia-CSIC, E-46071 Valencia, Spain
⁷⁵University of Victoria, Victoria, British Columbia, Canada V8W 3P6
⁷⁶Department of Physics, University of Warwick, Coventry CV4 7AL, United Kingdom
⁷⁷University of Wisconsin, Madison, Wisconsin 53706, USA

(Received 18 August 2011; published 21 November 2011)

We search for hadronic decays of a light Higgs boson (A^0) produced in radiative decays of an $Y(2S)$ or $Y(3S)$ meson, $Y \rightarrow \gamma A^0$. The data have been recorded by the *BABAR* experiment at the $Y(3S)$ and $Y(2S)$ center-of-mass energies and include $(121.3 \pm 1.2) \times 10^6$ $Y(3S)$ and $(98.3 \pm 0.9) \times 10^6$ $Y(2S)$ mesons. No significant signal is observed. We set 90% confidence level upper limits on the product branching fractions $\mathcal{B}(Y(nS) \rightarrow \gamma A^0) \mathcal{B}(A^0 \rightarrow \text{hadrons})$ ($n = 2$ or 3) that range from 1×10^{-6} for an A^0 mass of $0.3 \text{ GeV}/c^2$ to 8×10^{-5} at $7 \text{ GeV}/c^2$.

DOI: 10.1103/PhysRevLett.107.221803

PACS numbers: 14.80.Da, 12.60.Fr, 13.20.Gd, 14.40.Pq

A light CP -odd Higgs boson is expected in extensions to the standard model such as nonminimal supersymmetry [1]. Light, in this context, means a mass less than that of the $Y(1S)$ meson. Such a Higgs boson could be produced in radiative decays of the $Y(nS)$ mesons [2], $Y(nS) \rightarrow \gamma A^0$, where, in this analysis, $n = 2$ or 3 . *BABAR* has previously searched for this process where the A^0 decays to muons [3], taus [4], or invisibly [5,6]. CLEO has used its $Y(1S)$ data

sample to search in the muon-pair and tau-pair final states [7]. *BABAR* has also searched for violations of lepton universality in $Y(1S)$ decay [8], which could arise if the A^0 has the expected quantum numbers $J^{PC} = 0^{-+}$ and mixes with the $\eta_b(1S)$ [9].

Supersymmetry models in which $\tan^2 \beta$ is not small predict that the A^0 will decay predominantly into the heaviest kinematically available down-type fermion pair.

The earlier experimental results have ruled out much of the parameter space [10,11]. Regions not excluded tend to be dominated by hadronic decays, including decays to gluon pairs, gg , at smaller $\tan^2\beta$, and to charm quark pairs, $c\bar{c}$, at higher A^0 mass.

This analysis searches for hadronic decays of the A^0 in the mass range $2m_\pi < m_{A^0} < 7 \text{ GeV}/c^2$ without attempting to specify the underlying partons to which the A^0 decays. The analysis nominally assumes that the A^0 is CP -odd but also relaxes this assumption to obtain results without specifying the CP state.

The data were collected by the *BABAR* detector [12] at the PEP-II asymmetric-energy e^+e^- collider at the SLAC National Accelerator Laboratory. They consist of 27.9 fb^{-1} at the center-of-mass (c.m.) energy of the $Y(3S)$ and 13.6 fb^{-1} at the $Y(2S)$, corresponding to $N_{3S} = (121.3 \pm 1.2) \times 10^6$ $Y(3S)$ and $N_{2S} = (98.3 \pm 0.9) \times 10^6$ $Y(2S)$ mesons. We also use a continuum [i.e., non- $Y(nS)$] background sample consisting of 78.3 fb^{-1} of data collected at the c.m. energy of the $Y(4S)$, plus 11.8 fb^{-1} of data recorded 30–40 MeV below the $Y(2S)$, $Y(3S)$, or $Y(4S)$ c.m. energies. All of the data used here were recorded after the installation of an upgraded muon identification system [13].

Simulated signal events with various A^0 masses are used in the analysis. The EVTGEN event generator [14] is used to simulate particle decays. The A^0 is simulated as a spin-0 particle, with equal branching fractions to whichever of gg , $s\bar{s}$, and $c\bar{c}$ are kinematically available. Simulated events are produced both with and without the assumption that the A^0 is CP -odd. JETSET [15] is used to hadronize the partons, and GEANT4 [16] is used to simulate the detector response.

The search for the A^0 uses hadronic events in which the full event energy is reconstructed. The selection criteria were optimized using simulated signal events and the continuum data set. The highest-energy photon in each event is taken to be the radiative photon from the $Y(nS)$ decay. The A^0 candidate is constructed by adding the four-momenta of the remaining particles in the following order. The first added are $K_s^0 \rightarrow \pi^+\pi^-$ candidates that have mass within $25 \text{ MeV}/c^2$ of the true mass [17] and whose reconstructed vertices are separated from the interaction point by at least 3 times the uncertainty on the vertex location. Charged hadron identification is then used to assign the proton, K^\pm , or π^\pm mass to charged tracks. Tracks are labeled protons only if they are in the angular acceptance of the DIRC (Detector of Internally Reflected Cherenkov light) hadron identification system [12] and if there is another track identified as an antiproton. Neutral pion candidates are formed from pairs of photons, requiring the invariant mass of the photon pair to be between $100 \text{ MeV}/c^2$ and $160 \text{ MeV}/c^2$ and to have a π^0 energy greater than 200 MeV. Finally, any remaining unused photons are added. Photons, including those used to reconstruct π^0 mesons, are required to have a minimum energy of 90 MeV. All energies and momenta are in the c.m. frame.

Events are required to have a radiative photon energy greater than 2.5 GeV [$Y(3S)$] or 2.2 GeV [$Y(2S)$] and to have at least two charged tracks among the A^0 decay products. The A^0 mass resolution is improved by constraining the radiative photon and all A^0 decay products to come from a common vertex and the sum of the photon and A^0 four-momenta to be that of the c.m. system. To ensure that the full event energy is correctly reconstructed, the probability of the χ^2 of the constrained fit is required to be greater than a value that ranges from 0 at low A^0 mass to 0.01 at $m_{A^0} = 7 \text{ GeV}/c^2$. Events in which $m_{A^0} > 5 \text{ GeV}/c^2$ are rejected if the radiative photon, when combined with any other photon in the event, forms an invariant mass within $50 \text{ MeV}/c^2$ of the π^0 mass or, for $m_{A^0} > 6 \text{ GeV}/c^2$, within $50 \text{ MeV}/c^2$ of the η mass.

Additional criteria are used to reject radiative Bhabha events, $e^+e^- \rightarrow \gamma e^+e^-$, or radiative muon pairs, $e^+e^- \rightarrow \gamma\mu^+\mu^-$. An event is rejected if it was identified as a Bhabha at the trigger level, if either of the two highest-momentum tracks is identified as an electron or a muon, or if the angle between the radiative photon and the second-highest-momentum track is less than 1 rad. These criteria reject 96% of the continuum sample at a cost of 10–20% in signal efficiency and, according to simulation, reduce these backgrounds to negligible levels.

The analysis proceeds along two parallel paths labeled “ CP -all,” in which no assumption is made on the CP nature of the A^0 , and “ CP -odd,” in which it is assumed to be CP -odd. Events in which the A^0 decays to $\pi^+\pi^-$ or K^+K^- are excluded from the CP -odd analysis.

The analysis selects 371 740 events (CP -all) or 171 136 events (CP -odd) in the combined $Y(2S)$ and $Y(3S)$ (“on-peak”) data set with $0.29 < m_{A^0} < 7.1 \text{ GeV}/c^2$ (Fig. 1).

An A^0 signal would appear as a narrow peak in the candidate mass spectrum. The number of signal events at a particular hypothesis mass is computed as the number of events in a mass range (“window”) centered on that value, less the number of background events in the window. The width of the window depends on the A^0 mass resolution and was optimized along with the other selection criteria. It varies for CP -all from 3 to 26 MeV/c^2 as m_{A^0} increases from 0.29 to 7 GeV/c^2 . The CP -odd windows are the same width as CP -all above 2 GeV/c^2 but are larger at lower masses.

Background events are from $Y(nS)$ decays and from continuum. Continuum, which is dominant, mostly consists of the initial-state radiation (ISR) production of a light vector meson (clearly visible in Fig. 1) and nonresonant hadrons. The $Y(nS)$ backgrounds are primarily radiative decays to a light meson or nonresonant hadrons. At the highest A^0 candidate masses, there is an additional contribution from hadronic $Y(nS)$ decays in which a π^0 daughter is misidentified as the radiative photon. Simulation indicates that the fraction of $B\bar{B}$ events satisfying the selection

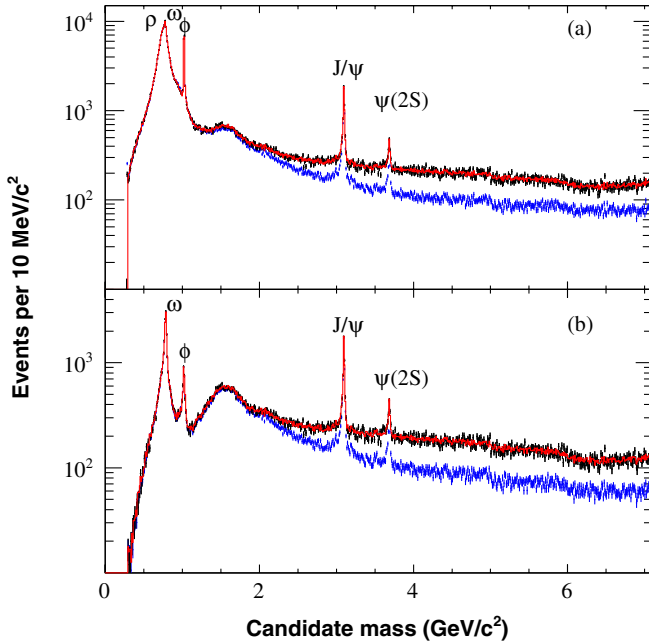


FIG. 1 (color online). Candidate mass spectrum in the (a) CP -all and (b) CP -odd analyses. The top curve in each plot is the on-peak data overlaid (in red) with the background fit described in the text, while the bottom curve (blue) is the scaled continuum data. The prominent initial-state radiation resonances are labeled.

criteria is negligible, so events recorded at the $Y(4S)$ c.m. energy can be used in the continuum sample.

The number of background events is obtained from a fit to the data that contains three components: continuum, nonresonant $Y(nS)$ radiative decay, and resonant $Y(nS)$ radiative decay. The continuum component is the candidate mass spectrum of the continuum data set multiplied by a normalization factor C_N (≈ 0.5). Because the efficiency for detecting the ISR photon depends on c.m. energy, C_N is not simply the ratio of integrated luminosities. It is left as a free parameter in the nominal fit but, as described below, is fixed to a calculated value for systematic studies. The nonresonant $Y(nS)$ component is a 16-knot cubic spline, fixed to 0 at the minimum A^0 mass. The resonant component includes five relativistic Breit-Wigner functions to represent the resonances for which CLEO saw some evidence in the study of $Y(1S) \rightarrow \gamma h^+ h^-$ ($h = \pi$ or K) [18]: $f_0(980)$, $f_2(1270)$, $f_2'(1525)$, $f_0(1710)$, and $f_4(2050)$. The masses and widths are fixed [17], and possible interference between the resonances is neglected in the fit. These resonances are all broad compared to an A^0 signal. The spacing of the knots, typically $0.5 \text{ GeV}/c^2$, is large enough that the cubic spline cannot conform to a narrow resonance.

The background fit (Fig. 1) has 21 free parameters and is made to 1362 bins of width $5 \text{ MeV}/c^2$, ranging from 0.29 to $7.1 \text{ GeV}/c^2$. The fit χ^2 are 1268 (CP -all) and 1293 (CP -odd) for 1341 degrees of freedom. Subtracting the normalized continuum mass spectrum from both the data

and the fit gives the $Y(nS)$ decay spectrum and the non-resonant and resonant radiative Y decay components of the fit (Fig. 2).

The uncertainty on the background in each mass window is both statistical and systematic. The systematic error is the sum in quadrature of the change in the total background arising from each of 17 alternative fits: the five nominal light resonances are removed one at a time, and 11 additional resonances are included one at a time. The 11 are established resonances [17] with even total angular momentum, charge conjugation quantum number of $+1$, and isospin 0. The 17th alternative fit is performed with C_N fixed to the midpoint of the range of values found from four different methods of determining it. Two of the methods are the nominal fits to the CP -odd and CP -all samples, and two use ISR-produced narrow resonances in four different final states: $e^+e^- \rightarrow \gamma\omega$, $\omega \rightarrow \pi^+\pi^-\pi^0$; $e^+e^- \rightarrow \gamma\phi$, $\phi \rightarrow K^+K^-$; $e^+e^- \rightarrow \gamma J/\psi$, $J/\psi \rightarrow \geq 4$ charged tracks, with no π^0 ; and $e^+e^- \rightarrow \gamma J/\psi$, $J/\psi \rightarrow \geq 4$ charged tracks, with one π^0 . First, the number of each of these resonances is compared in on-peak and continuum data. Second, the same ratios are obtained using simulated samples of these ISR events, together with the calculated production cross sections [19] and the recorded luminosities. The resulting value of C_N is 4.5% larger than nominal for CP -all and 2.7% for CP -odd. The fit qualities are good in all alternative fits. The systematic errors are small compared to statistical errors, except near resonances.

The A^0 signal is evaluated at hypothesis masses that range from $0.291 \text{ GeV}/c^2$ to $7.000 \text{ GeV}/c^2$ in $1 \text{ MeV}/c^2$

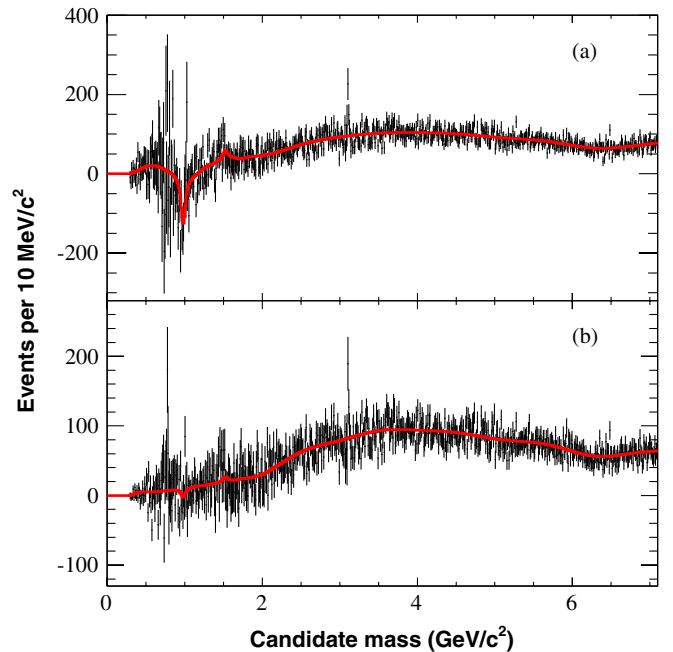


FIG. 2 (color online). A^0 candidate mass spectrum after continuum subtraction, overlaid with fit. (a) CP -all analysis; (b) CP -odd analysis.

steps for the CP -all analysis (6710 mass hypotheses) and from 0.300 GeV/c^2 to 7.000 GeV/c^2 in 1 MeV/c^2 steps for CP -odd (6701 masses). Figure 3 shows the nominal statistical significance of the resulting A^0 signal, defined as the number of events divided by the statistical error, as a function of mass. The largest upwards fluctuations are 3.5σ at 3.107 GeV/c^2 for CP -all and 3.2σ at 0.772 GeV/c^2 for CP -odd. Including background systematic errors, the significance of these two, which are located near the J/ψ and ρ resonances, respectively, are reduced to 2.8σ and 2.2σ . The largest remaining fluctuations are 2.9σ at 1.295 GeV/c^2 for CP -all and 3.1σ at 4.727 GeV/c^2 for CP -odd. Figure 4 histograms the statistical significance of the signal measured at each mass, overlaid with the distribution expected in the absence of a signal.

The signal extraction technique is studied using many simulated experiments. Each experiment consists of two candidate mass distributions, one for on-peak data and the other for continuum. The continuum event distributions are obtained from the full $Y(4S)$ data, which is 11 times larger than the on-peak data set. The nonresonant $Y(nS)$ events are generated from a smooth threshold curve, and the resonant events are generated from relativistic Breit-Wigner functions. The full signal extraction is then performed. The average bias on the A^0 signal yield is less than 1.5 events for all masses when there is no signal.

These studies are also used to calculate the expected distribution of statistical significance in the absence of signal (Fig. 4) and to evaluate the significance of the largest

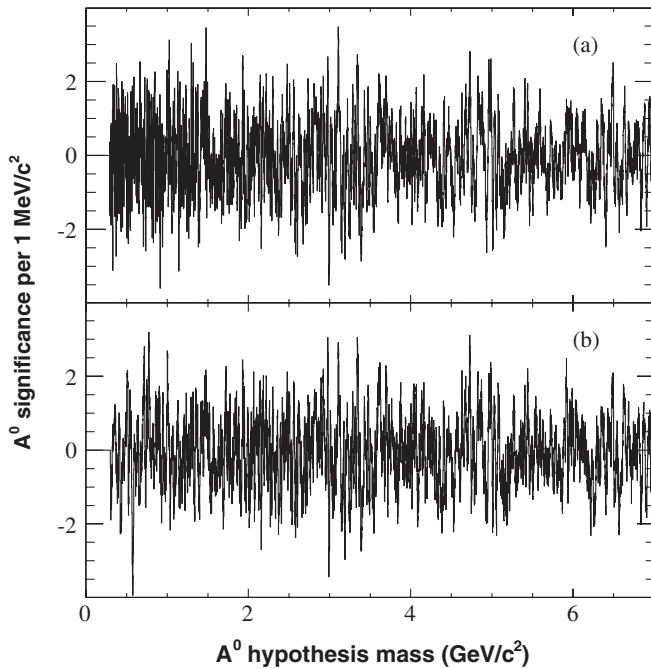


FIG. 3. Statistical significance (events divided by statistical error) of the A^0 signal as a function of mass, for (a) CP -all analysis and (b) CP -odd analysis.

apparent A^0 signals. The fraction of background-only CP -all simulated experiments that contain a fluctuation of nominal statistical significance $\geq 3.5\sigma$ is 33%. The fraction of CP -odd simulated experiments that contain a fluctuation $\geq 3.2\sigma$ is 63%. We therefore see no evidence of signal. The studies further indicate that large correlations between the resonant and nonresonant $Y(nS)$ components make the uncertainties on the yields of the resonances unreliable.

In the absence of a significant signal, we calculate a 90% confidence level (C.L.) upper limit for each hypothesis mass on the product branching fractions $\mathcal{B}_{3S} \equiv \mathcal{B}(Y(3S) \rightarrow \gamma A^0) \mathcal{B}(A^0 \rightarrow \text{hadrons})$ and $\mathcal{B}_{2S} \equiv \mathcal{B}(Y(2S) \rightarrow \gamma A^0) \mathcal{B}(A^0 \rightarrow \text{hadrons})$, assuming that the $Y(3S)$ and $Y(2S)$ decays are described by the same matrix element. This implies that $\mathcal{B}_{2S} = \mathcal{B}_{3S} \Gamma_{3S} / \Gamma_{2S} R(m_{A^0})$, where Γ_{3S} and Γ_{2S} are the full widths of the $Y(3S)$ and $Y(2S)$, respectively, and R accounts for the difference in phase space. R is within a few percent of unity for all A^0 masses.

The calculation uses the relationship $\hat{N} = \hat{B} + N'_{3S} \mathcal{B}_{3S} \epsilon$, where \hat{N} is the expected number of observed events for the given value of \mathcal{B}_{3S} , \hat{B} is the expected background, $N'_{3S} \equiv N_{3S} + N_{2S} \Gamma_{3S} / \Gamma_{2S} R(m_{A^0})$, and ϵ is the signal efficiency. We calculate a likelihood $\mathcal{L}(\mathcal{B}_{3S})$, defined as the probability of observing N or fewer events given that value of \mathcal{B}_{3S} where N is the number actually observed. $\mathcal{L}(\mathcal{B}_{3S})$ is obtained by integrating over the uncertainties in \hat{B} , N_{2S} , N_{3S} , and ϵ , which are assumed to be Gaussian. The 90% C.L. upper limit \mathcal{B}_{90} is calculated assuming a uniform prior above 0: $\int_0^{\mathcal{B}_{90}} \mathcal{L}(\mathcal{B}_{3S}) d\mathcal{B}_{3S} = 0.90 \int_0^\infty \mathcal{L}(\mathcal{B}_{3S}) d\mathcal{B}_{3S}$.

The efficiency is calculated using simulated events. The efficiency for the CP -all analysis ranges from a peak of 22% near $m_{A^0} = 0.6 \text{ GeV}/c^2$ to less than 1% at high

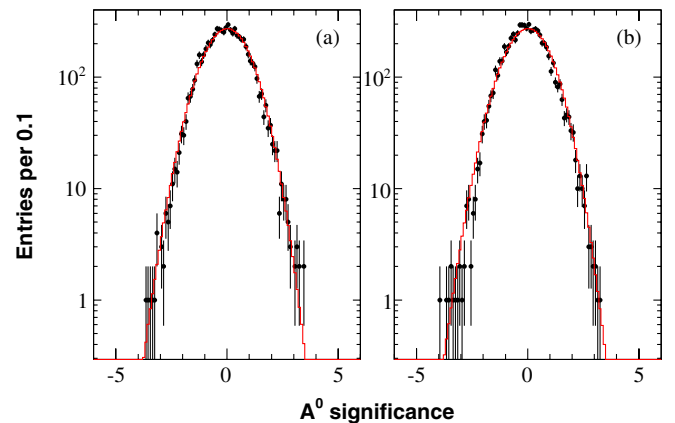


FIG. 4 (color online). Histogram of the statistical significance of the A^0 signal for (a) the 6710 masses considered in the CP -all analysis and for (b) the 6701 masses in the CP -odd analysis. The overlaid curve shows the distribution expected in the absence of signal.

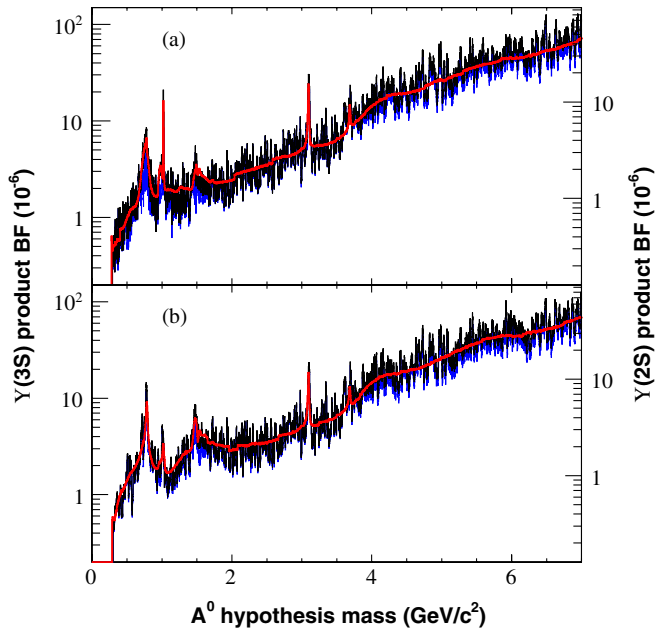


FIG. 5 (color online). 90% C.L. upper limits on product branching fractions (BF) (left axis) $\mathcal{B}(Y(3S) \rightarrow \gamma A^0) \mathcal{B}(A^0 \rightarrow \text{hadrons})$ and (right axis) $\mathcal{B}(Y(2S) \rightarrow \gamma A^0) \mathcal{B}(A^0 \rightarrow \text{hadrons})$, for (a) CP -all analysis and (b) CP -odd analysis. The overlaid curves (red online) are the limits expected from simulated experiments, while the light gray curves (blue online) are the limits from statistical errors only. The $Y(2S)$ limits do not include the phase space factor, which is at most a 3.5% correction.

masses, while, for the CP -odd analysis, it ranges from 12% near 0.9 GeV/c^2 to less than 1% at high masses.

The uncertainty on the efficiency is typically 11% (CP -all) or 7% (CP -odd) below the $c\bar{c}$ threshold and 25% above. This includes contributions from uncertainty in tracking (1.5–3.5% depending on mass), photon and π^0 reconstruction (5–10%), and particle identification (3–5%), but the dominant contribution is due to the A^0 decay branching fractions. This uncertainty is evaluated by varying the assumed branching fractions. Below the $c\bar{c}$ threshold, it is changed from 50% $s\bar{s}$ and 50% $g\bar{g}$ to 100% $g\bar{g}$. Above the $c\bar{c}$ threshold, it is changed from one-third each $g\bar{g}$, $s\bar{s}$, and $c\bar{c}$ to 50% $c\bar{c}$, 25% $g\bar{g}$, and 25% $s\bar{s}$. The resulting systematic errors are 8% for CP -all or 4% for CP -odd below the $c\bar{c}$ threshold and 21% above. The resulting 90% C.L. upper limits are shown in Fig. 5.

In conclusion, we have searched for hadronic final states of a light Higgs boson produced in radiative decays of the $Y(2S)$ or $Y(3S)$ and find no evidence of a signal. Upper limits on the product branching fraction $\mathcal{B}(Y(nS) \rightarrow \gamma A^0) \mathcal{B}(A^0 \rightarrow \text{hadrons})$ range from 1×10^{-6} at 0.3 GeV/c^2 to 8×10^{-5} at 7 GeV/c^2 at the 90% C.L.

We are grateful for the excellent luminosity and machine conditions provided by our PEP-II colleagues and for the substantial dedicated effort from the computing organizations that support *BABAR*. The collaborating institutions

wish to thank SLAC for its support and kind hospitality. This work is supported by DOE and NSF (USA), NSERC (Canada), IHEP (China), CEA and CNRS-IN2P3 (France), BMBF and DFG (Germany), INFN (Italy), FOM (The Netherlands), NFR (Norway), MIST (Russia), and PPARC (United Kingdom). Individuals have received support from CONACyT (Mexico), A. P. Sloan Foundation, Research Corporation, and Alexander von Humboldt Foundation.

*Present address: Temple University, Philadelphia, PA 19122, USA.

†Also at Università di Perugia, Dipartimento di Fisica, Perugia, Italy.

‡Present address: University of Huddersfield, Huddersfield HD1 3DH, UK.

§Present address: University of South Alabama, Mobile, AL 36688, USA.

||Also at Università di Sassari, Sassari, Italy.

- [1] R. Dermisek and J. F. Gunion, *Phys. Rev. Lett.* **95**, 041801 (2005).
- [2] R. Dermisek, J. F. Gunion, and B. McElrath, *Phys. Rev. D* **76**, 051105(R) (2007).
- [3] B. Aubert *et al.* (*BABAR* Collaboration), *Phys. Rev. Lett.* **103**, 081803 (2009).
- [4] B. Aubert *et al.* (*BABAR* Collaboration), *Phys. Rev. Lett.* **103**, 181801 (2009).
- [5] B. Aubert *et al.* (*BABAR* Collaboration), [arXiv:0808.0017](https://arxiv.org/abs/0808.0017).
- [6] P. del Amo Sanchez *et al.* (*BABAR* Collaboration), *Phys. Rev. Lett.* **107**, 021804 (2011).
- [7] W. Love *et al.* (CLEO Collaboration), *Phys. Rev. Lett.* **101**, 151802 (2008).
- [8] P. del Amo Sanchez *et al.* (*BABAR* Collaboration), *Phys. Rev. Lett.* **104**, 191801 (2010).
- [9] F. Domingo, U. Ellwanger, E. Fullana, C. Hugonie, and M.-A. Sanchis-Lozano, *J. High Energy Phys.* **01** (2009) 061.
- [10] R. Dermisek and J. F. Gunion, *Phys. Rev. D* **81**, 075003 (2010).
- [11] F. Domingo, *J. High Energy Phys.* **04** (2011) 016.
- [12] B. Aubert *et al.* (*BABAR* Collaboration), *Nucl. Instrum. Methods Phys. Res., Sect. A* **479**, 1 (2002).
- [13] M. Andreotti *et al.* (*BABAR* LST Collaboration), SLAC National Laboratory Report No. SLAC-PUB-12205, 2005.
- [14] D. J. Lange, *Nucl. Instrum. Methods Phys. Res., Sect. A* **462**, 152 (2001).
- [15] T. Sjostrand, [arXiv:hep-ph/9508391](https://arxiv.org/abs/hep-ph/9508391).
- [16] S. Agostinelli *et al.* (GEANT4 Collaboration), *Nucl. Instrum. Methods Phys. Res., Sect. A* **506**, 250 (2003).
- [17] K. Nakamura *et al.* (Particle Data Group), *J. Phys. G* **37**, 075021 (2010).
- [18] S. B. Athar *et al.* (CLEO Collaboration), *Phys. Rev. D* **73**, 032001 (2006).
- [19] M. Benayoun, S. I. Eidelman, V. N. Ivanchenko, and Z. K. Silagadze, *Mod. Phys. Lett. A* **14**, 2605 (1999).